

# Performance of low-loss demountable joints between CORC<sup>®</sup> cable-in-conduit-conductors at magnetic fields up to 8 T developed for fusion magnets

Jeremy D Weiss<sup>1,2,\*</sup> , Danko C van der Laan<sup>1,2</sup> , Kyle Radcliff<sup>1</sup>, Nadezda Bagrets<sup>3</sup> , Christian Lange<sup>3</sup>, Steven Allen<sup>4</sup>, Julian Holt<sup>4</sup>, Ian Alsworth<sup>4</sup>, Peter Daniels<sup>4</sup>, Yannik Dieudonne<sup>4</sup> and Frank Schoofs<sup>4</sup>

<sup>1</sup> Advanced Conductor Technologies LLC, Boulder, CO 80301, United States of America

<sup>2</sup> Department of Physics, University of Colorado, Boulder, CO 80309, United States of America

<sup>3</sup> Institute for Technical Physics—IATEP, Karlsruhe Institute of Technology, Karlsruhe, Germany

<sup>4</sup> United Kingdom Atomic Energy Authority, Culham Science Centre, Abingdon, Oxfordshire, United Kingdom

E-mail: [Jeremydavidweiss@gmail.com](mailto:Jeremydavidweiss@gmail.com)

Received 7 March 2023, revised 31 May 2023

Accepted for publication 6 June 2023

Published 16 June 2023



CrossMark

## Abstract

High-temperature superconductors (HTS) are promising candidates for use in the high-field magnets needed in particle accelerators and fusion reactors. HTS conductor on round core (CORC<sup>®</sup>) cables and wires wound from ReBa<sub>2</sub>Cu<sub>3</sub>O<sub>7-x</sub> (REBCO) coated tapes are being developed for use in high-field magnet applications including fusion magnets operating at currents beyond 80 kA, requiring them to be bundled into cable-in-conduit conductor (CICC) configurations. The use of HTS cables enable demountable superconducting fusion magnets that would allow easier access to the fusion machine for maintenance and parts replacement. Such demountable magnets require practical, low-resistance joints, capable of injecting current uniformly into the many REBCO tapes that make up different cable designs. Optimization steps on CORC<sup>®</sup> cables have resulted in high-current terminations and joints with a joint resistance measured between a pair of 30-tape CORC<sup>®</sup> cables of 51 nΩ at 76 K and 1.9 nΩ at 4 K. Demountable joints between CICC consisting of six CORC<sup>®</sup> cables arranged in flat and round configurations were also tested and compared to joints between low-temperature superconducting (LTS) CICC consisting of NbTi Rutherford cables. Samples were paired into two configurations (LTS-to-LTS and HTS-to-HTS) with a demountable joint between them that were each tested in series with currents up to 10 000 A in an applied background magnetic field of up to 8 T. The total loop resistance of the HTS-to-HTS sample, including their terminations and joint, was about 4 nΩ at 4 K in self-field with the resistance of the copper pressed joint being less than 1 nΩ. At 8 T, the total loop resistance increased to 6.9 nΩ with the pressed joint contributing 1.4 nΩ. These initial tests prove the feasibility of producing remountable (dry) joints with low resistance between superconducting magnet windings in future compact fusion machines.

\* Author to whom any correspondence should be addressed.

Keywords: demountable, joints, CORC<sup>®</sup>, CICC, fusion cables, HTS, REBCO

(Some figures may appear in colour only in the online journal)

## 1. Introduction

High-temperature superconductors (HTS) are promising candidates for use in fusion magnets, in particular for compact fusion machines that operate at high fields that are inaccessible using low-temperature superconductors (LTS) [1]. The high critical fields and critical temperatures of HTS allow them to operate at magnetic fields significantly above 20 T and temperatures exceeding 10 K. High current HTS cables are essential for the success of compact fusion reactors such as affordable, robust, compact reactor (ARC) and soonest possible ARC (SPARC) proposed by the Massachusetts Institute of Technology [2] and now being developed by Commonwealth Fusion Systems [3], compact high-field tokamak magnets under development at Tokamak Energy Ltd [4], and the advanced beam-driven field reversed configuration reactors under development at Tri Alpha Energy Technologies [5]. The possibility to operate HTS magnets under higher heat loads at higher temperatures, compared to LTS, enables demountable magnets [2] in which the magnet windings contain separable joints. Demountable fusion magnets are of high interest because they enable rapid reconfiguration and servicing of the machine that is otherwise a significant challenge in tokamaks that cannot be disassembled [6]. Demountable fusion magnets are being considered in ARC, the fusion nuclear science facility (FNSF) under development at the Princeton Plasma Physics Laboratory [7], and the spherical tokamak for energy production fusion machine for which development was authorized only recently by the United Kingdom Atomic Energy Authority (UKAEA) [8]. The brief, and likely incomplete overview of compact fusion machines that are currently under development clearly shows that HTS have become an enabling technology for fusion energy science that may lead to fusion energy production.

The success of the various compact fusion machines depends on the development of reliable high-current HTS conductors that will not degrade under the high operating stresses, the ability to inject current evenly into the HTS cables, and to make reliable, low-resistant joints between the cables. A prime example of the importance of joints between high-current superconducting cables is the failure of a joint in the large hadron collider (LHC) at the European Organization for Nuclear Research (CERN), where a single malfunctioning joint caused damage to the LHC magnets and cryogenic system in the order of \$21 M while causing a delay in commissioning the LHC for 12 months [9]. The failure of this soldered joint between magnet leads emphasizes the challenge in developing demountable toroidal field (TF) coils in which each winding contains two pressed joints that are not soldered. The resistance of each joint needs to be below about 5 n $\Omega$  at the operating temperature as high as 30 K, while experiencing a background magnetic field of several Tesla. Even a joint with 1 n $\Omega$  resistance would

dissipate 2.5 W at an operating current of 50 kA. Excessive dissipation at the joint could easily overwhelm the cooling of the joint, especially when cooled through conduction or by helium gas, resulting in a hot spot and potentially a magnet quench.

Here we report on the development of demountable joints between cable-in-conduit conductor (CICC) made from conductor on round core (CORC<sup>®</sup>) cables, developed by advanced conductor technologies (ACT) [10]. CORC<sup>®</sup> cables are an attractive option for HTS fusion magnets. CORC<sup>®</sup>-CICC have been developed for TF coils that would allow operation at currents exceeding 80 kA at 4 K and 20 T [11–13]. ACT developed low-resistance CORC<sup>®</sup> cable terminations that ensure even current distribution between the ReBa<sub>2</sub>Cu<sub>3</sub>O<sub>7-x</sub> (REBCO) tapes in the cable by trimming the tape layers, allowing direct contact of each tape with the copper termination [14, 15]. Even current distribution between tapes is needed to minimize the contact resistance of the cable terminations and for ensuring that the cable can be operated at its full capacity [16]. Demountable CORC<sup>®</sup>-CICC joints, in which the joints are formed by pressing the copper terminations of the CORC<sup>®</sup>-CICC together, are developed and their contact resistance is measured at 4 K in a background field of up to 8 T at currents up to 10 kA. Emphasis is given on factors that affect joint resistance including terminal heating temperature and duration, as well as the clamping structure needed to provide sufficient contact pressure between the copper joint surfaces. The results provide a roadmap for developing reliable, low-resistance joints between HTS CICC that would enable demountable TF coils in future fusion reactors.

## 2. Experimental methods

### 2.1. Resistance measurements of copper joint components and solder joints between superconducting tapes

The resistivity of copper joint components was measured by a standard four-point transport measurement using 100 mm long sections of material with a cross-section of approximately 6 mm<sup>2</sup>. The sections were cut from joint and terminals of the test samples. A current of 1 or 2 A was applied while the voltage was measured at room temperature (293 K), in boiling liquid nitrogen (76 K), and in boiling liquid helium (4 K) using a Keithley 2182 A nanovoltmeter. The copper sections were tested both in the as-received condition (typically 1/2 or 3/4 hard) and after annealing at 450 °C for 2.5 h and 575 °C for 2 h in a mixture of 95% Ar and 5% H<sub>2</sub> gas. All copper hardware used to manufacture the joints of the various samples was annealed under these conditions.

The tapes chosen for cable winding were 4 mm wide SCS4050-AP REBCO tapes manufactured by Superpower Inc. The tapes contained a Hastelloy substrate of 50  $\mu$ m thickness and were surround plated with a 5  $\mu$ m thick copper

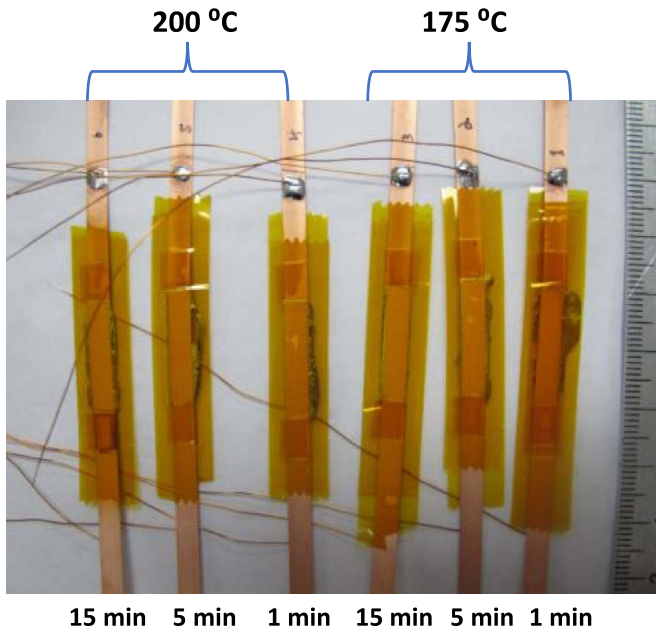


**Figure 1.** Lap-joints prepared between REBCO tapes.

layer. The contact resistance of the solder joint between two REBCO tapes was measured to determine the effect of temperature and time at which the joint was prepared on the joint resistance. Excessive heating time and temperature could potentially affect the internal contact resistance of the REBCO tapes [17, 18]. Therefore, 20 mm long face-to-face lap joints were prepared (figure 1) by cleaning the surfaces with acetone and flux, applying a  $4 \times 20$  mm strip of indium foil (0.18 mm thick) between the tapes, and then heating to either 175 °C or 200 °C while applying a constant force using a weight of 58 g. The voltage was then measured across the joint as a function of current ( $V(I)$ ) at 76 K via a standard four-point transport measurement (see equation in [19]) and the critical current ( $I_c$ ) was determined using an electric field criterion of  $1 \mu\text{Vcm}^{-1}$ .

## 2.2. Design and testing of joints between single CORC<sup>®</sup> cables

Two different CORC<sup>®</sup> cable designs were manufactured, one containing 30 tapes to study a joint between a single cable (CORC<sup>®</sup>-30), and another with 12 tapes (CORC<sup>®</sup>-12) that was used to manufacture CICC samples containing six CORC<sup>®</sup> cables each. Table 1 shows the properties of the two cables, both of which include a 50  $\mu\text{m}$  thick polyester insulating layer.

A section of cable CORC<sup>®</sup>-30 with 89 cm length between terminals was tested at the Karlsruhe Institute of Technology within a 12 T split-pair LTS magnet. The sample was mounted in an insulating G10 sample holder that included a 9 cm long clam-shell copper block with Kapton heater strips in the center of the holder. Temperature sensors were included at

**Table 1.** Properties of the two CORC<sup>®</sup> cables studied.

|                                      |      | CORC <sup>®</sup> -12 | CORC <sup>®</sup> -30 |
|--------------------------------------|------|-----------------------|-----------------------|
| Tape width                           | (mm) | 4                     | 4                     |
| # of tapes                           | (-)  | 12                    | 30                    |
| # of tape layers                     | (-)  | 4                     | 10                    |
| Average tape $I_c$ (77 K, SF)        | (A)  | 133                   | 121                   |
| Sum of average tape $I_c$ (77 K, SF) | (A)  | 1596                  | 3630                  |
| Cable outer diameter                 | (mm) | 5.98                  | 6.80                  |

three points within the copper block to measure the temperature of the block and to estimate the temperature of the cable, as described in [20]. Voltage was then measured across the terminations as a function of current at various applied fields up to 12 T and temperatures ranging from 4 K to 56 K. The critical current of the cable was then determined using an electric field criterion of  $1 \mu\text{Vcm}^{-1}$  with a length of 9 cm after subtracting the linear contribution of  $V(I)$  due to the contact resistance of the terminations.

Another section of cable CORC<sup>®</sup>-30 with 93 cm length between terminations was bent to a 12 cm diameter hairpin (see figure 2) and the  $V(I)$  characteristic was measured in boiling liquid nitrogen at 76 K and in boiling liquid helium at 4 K. The voltage was measured using voltage taps located within the terminations that also measured a portion of the contact resistance between the REBCO tapes and the terminations. The cable was then cut in half, the tape layers of the cable ends trimmed to form a tapered shape, and then soldered within a copper structure using indium solder to form a fixed joint measuring  $16 \times 38 \times 200$  mm. Details of the tapering and soldering process can be found in [10] and [12]. The  $V(I)$  tests were then repeated using the same voltage taps as before the joint was formed to accurately determine the joint resistance. The resistivity  $\rho$  of the copper used was  $0.13 \text{ n}\Omega \text{ m}$  at 4 K. This sample allowed measurement of the contact resistance between the CORC<sup>®</sup> cable and the copper joint structure, which will have a major impact on the overall resistance of demountable joints between CORC<sup>®</sup> CICC.

## 2.3. Design and testing of demountable CICC joints

Three CICC sample layouts were manufactured at ACT, one containing three NbTi Rutherford cables soldered into a copper jacket, one containing six CORC<sup>®</sup> cables placed into a flat ribbon-like arrangement, and one with six CORC<sup>®</sup> cables placed into a round arrangement. Schematics of each layout are presented in figure 3. Due to limitations of applied magnetic field and sample current, CORC<sup>®</sup> cables with only 12 tapes were used to match the rated current of 20 kA at 7 T in the NbTi CICC. The test samples were 610 mm long and consisted of an injection terminal, a jacketed CICC section, and a joint terminal section.

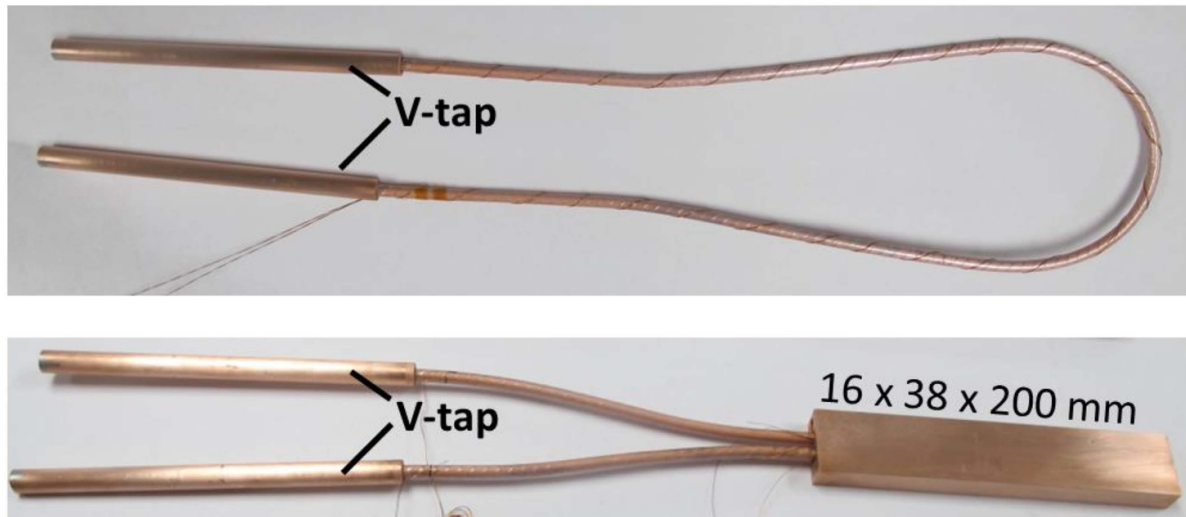


**Figure 2.** Picture of cable CORC®-30 with terminations after bending into a hairpin and after inserting a joint between the cut sample.

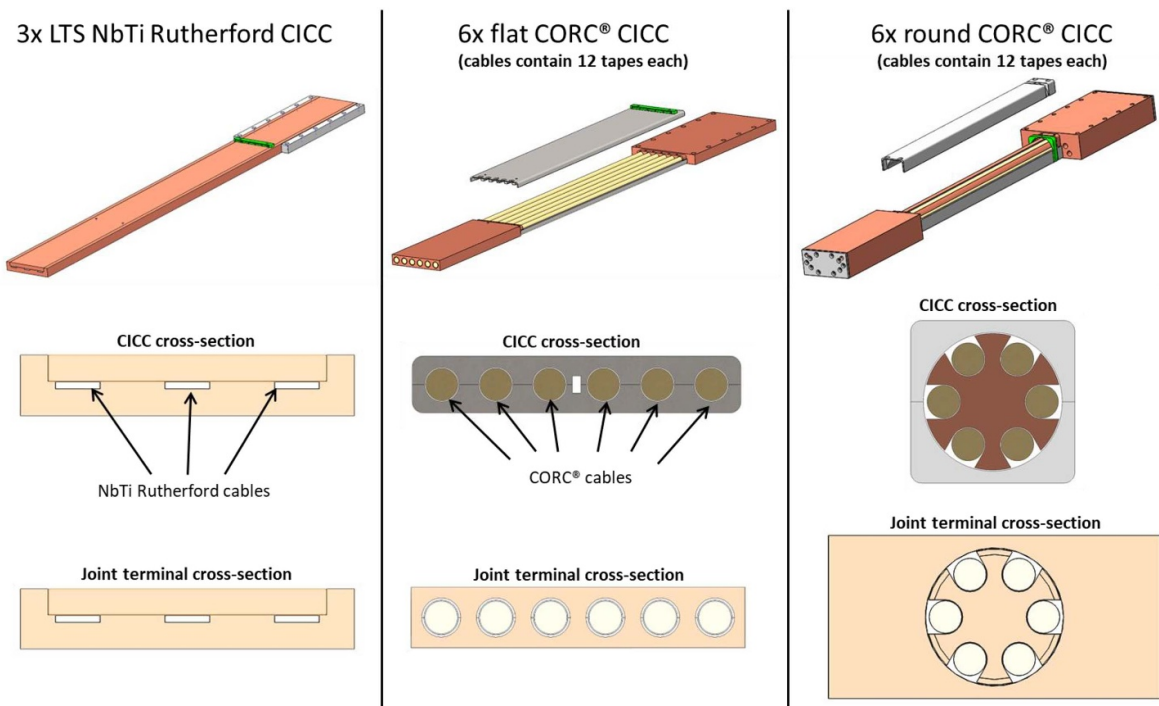


**Figure 3.** Overview of the three CICC layouts manufactured including an exploded view of the test samples and cross-sections of the CICCs as well as their terminations.

After testing the HTS-to-HTS sample, results were analyzed (see discussion) and it became apparent that the joint resistance was negatively influenced by two factors. First, the copper used in the manufacture of the round HTS sample was not actually the specified (99.99% pure) copper, having a measured resistance that was higher than expected and indicative of a low-purity copper or an alloy of copper. Second, the heating time used for soldering the CORC® cables within the joint and injection termination blocks was 20–45 min, which negatively impacts the contact resistance of the REBCO tapes. Therefore, a second pair of HTS samples was prepared

using verified high-purity copper and shorter soldering times of about 10 min.

Demountable joints between sample pairs were prepared using a clamping structure to create a dry copper-to-copper pressure contact between the terminals of the samples. The joint contact area between samples measured 150 mm × 61 mm. The demountable joint was inserted into an 8 T superconducting solenoid magnet with a 129 mm diameter bore and the  $V(I)$  characteristics were measured as a function of magnetic field applied along the length of the joint. The field homogeneity, defined as  $(B_{\text{joint}} - B_{\text{set}})/B_{\text{set}}$  where  $B_{\text{joint}}$  is the

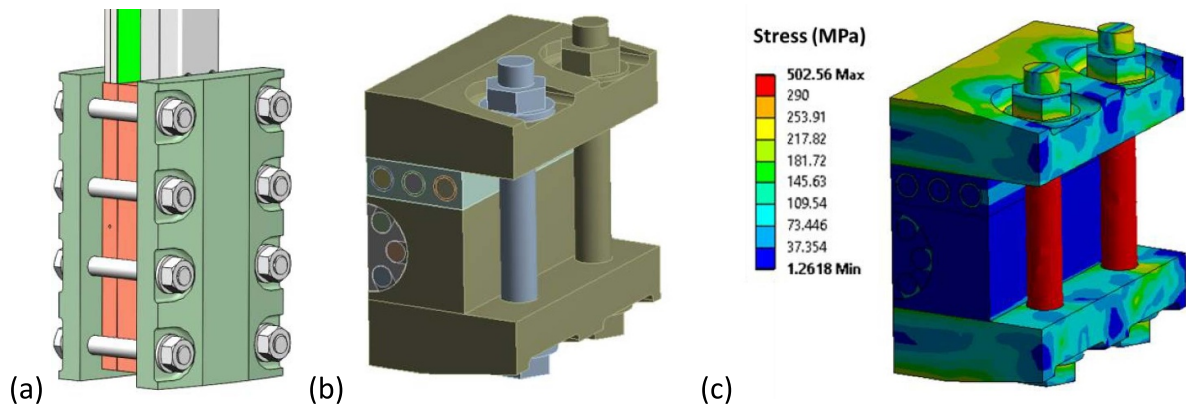


**Figure 4.** (a) Overview of the joint between two CICC samples containing the clamping plates. (b) Detailed view of the different components used in the ANSYS model. (c) Von-Mises stress in one quarter of the clamping plates and sample after a load of 40 kN was applied per bolt, followed by cool down to 4.2 K. The yield stress of the bolts is 900 MPa.

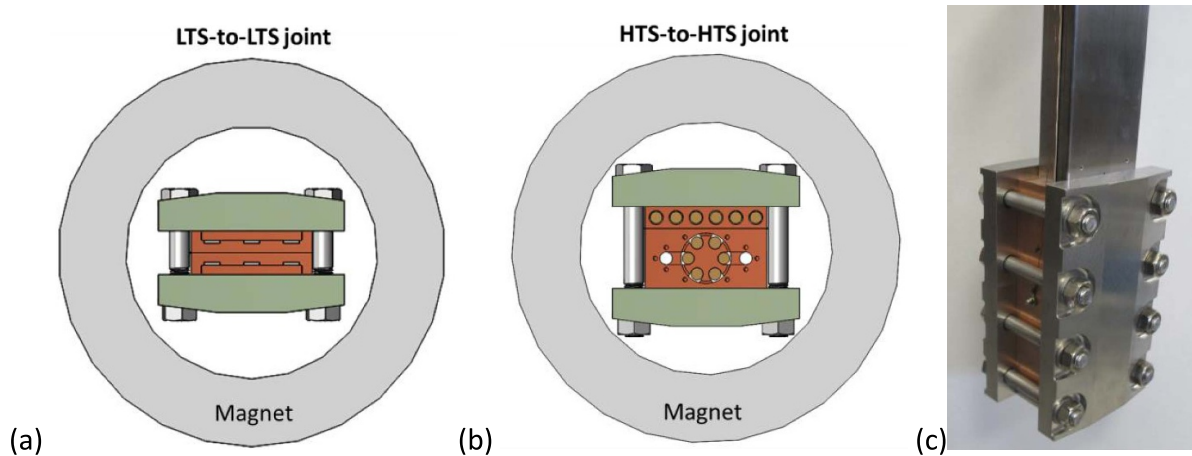


**Figure 5.** Schematics showing the joint configurations tested between (a) LTS samples and (b) HTS samples. (c) Picture of the HTS-to-HTS joint before inserting into the magnet bore.

field within any portion of the joint and  $B_{\text{set}}$  is the set applied field, was between  $-0.14$  and  $0.04$  within the joint.

The stainless steel joint clamping structure was designed to ensure an even contact pressure between dry copper-to-copper joint surfaces of at least 10 MPa while also fitting into the limited volume of the magnet. Detailed finite element method optimization of the clamping structure was performed using ANSYS software at the UKAEA to confirm this contact pressure could be achieved between samples without excessively stressing the CORC<sup>®</sup> cables within the joint or yielding any of the clamping hardware (see figure 4). Pressure sensitive Fuji<sup>®</sup> film was used to verify that the pressed contact area exceeded 10 MPa between samples.

#### 2.4. Testing of demountable CICC joints

The CICC samples were paired into two different test configurations. Two NbTi CICC samples formed the LTS-to-LTS configuration shown in figure 5(a). The two CORC<sup>®</sup> CICC samples formed the HTS-to-HTS configuration shown

in figures 5(b) and (c). As shown in figure 6, voltage was measured across six locations. The total sample voltage was measured across either samples' injection terminals, labelled V1 on the right (R) side of the terminals and V2 on the left (L) side of the terminals. Voltage pairs V3 and V4 measured the voltage between injection and joint terminals on the right and left side of the round CORC<sup>®</sup> CICC, respectively. Likewise, V5 and V6 measured the voltage between injection and joint terminals on the right and left side of the flat CORC<sup>®</sup> CICC. For the LTS-to-LTS sample pair, the total voltage was measured for the whole sample pair as well as for each sample, labeled sample 1(S1) and sample 2(S2). The voltage generated by the inductive ramping of current ( $V_0$ ) is defined as the y-intercept of linear fits of the  $V(I)$  data. The slope of the linear fits was used to determine resistance values for both right and left sides of the samples that were then averaged together to determine the total resistance ( $R_{\text{Total}}$ ) of the sample pair and the resistance for each sample leg ( $R_{\text{Round HTS1}}$ ,  $R_{\text{Round HTS2}}$ ,  $R_{\text{Flat HTS1}}$ ,  $R_{\text{Flat HTS2}}$ ,  $R_{\text{LTS1}}$ , and  $R_{\text{LTS2}}$ ). The joint resistances were then calculated for each sample pair by subtracting  $R_{\text{Total}}$

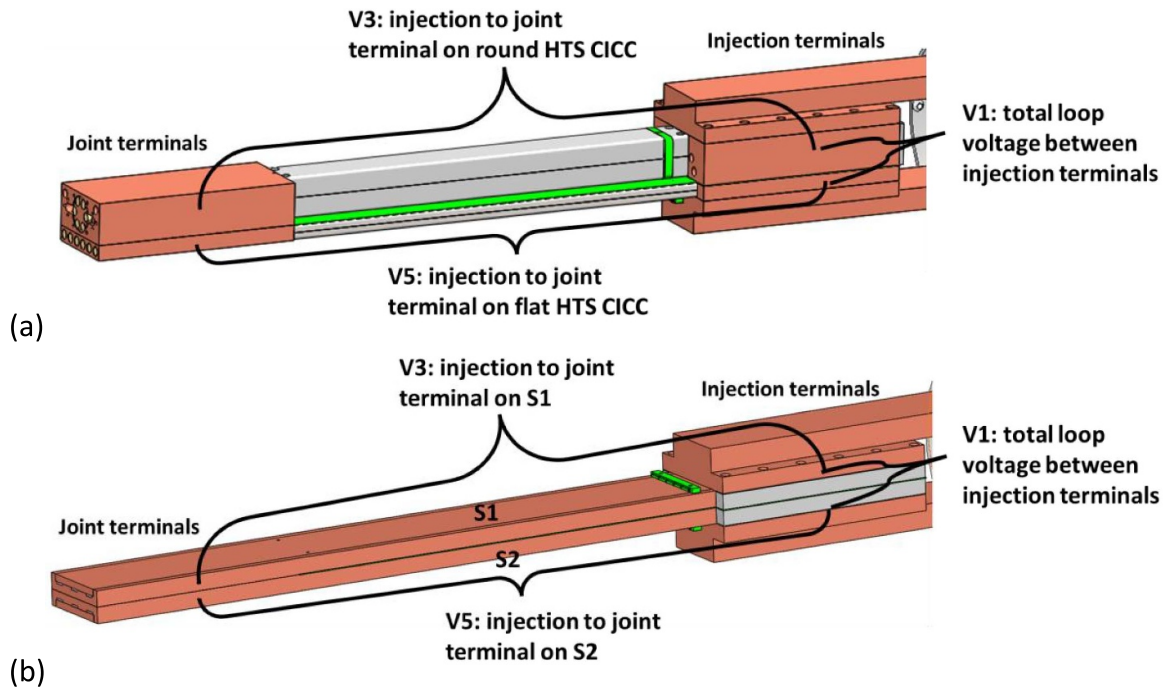


**Figure 6.** a. Overview of the joint formed by the two CICC samples and the location of some of the voltage pairs for (a) the HTS-to-HTS sample pair and (b) the LTS-to-LTS sample pair. For clarity, the clamping hardware at the joint terminals is not shown. A thin sheet of G10 insulation separates the injection terminals of either sample.

by the resistance measured over each of the sample legs (e.g.  $R_{\text{Joint}} = R_{\text{Total}} - R_{\text{Round HTS1}} - R_{\text{Flat HTS1}}$ ).

### 3. Results

#### 3.1. Performance of CORC® cables and single-cable joints

The critical current of cable CORC®-30, containing 30 REBCO tapes, was determined at Karlsruhe Institute of Technology as a function of applied magnetic field from 2–12 T at temperatures ranging from 4.2 K to 56 K. Figure 7 shows the general trend of decreasing  $I_c$  with increasing applied field and temperature. At 4 K, 12 T,  $I_c$  was 9 kA, decreasing to 5.5 kA at 25.6 K. A six-cable CICC configuration using cable CORC®-30 would therefore carry approximately 33 kA at 25.6 K, while a CICC using 50 tape CORC® cables would carry about 55 kA. Even higher currents could be achieved at these elevated temperatures by utilizing more CORC® cables in a CICC, or higher pinning tapes (e.g. ‘HM’ tapes from SuperPower Inc.) that have only just recently become available with  $I_c$  over two times higher than for the tapes used in this study [21].

Figure 8(a) shows the electric field ( $E$ ), defined as  $V$  divided by the length between the voltage taps, as a function of current for cable CORC®-30 pictured in figure 2. The voltage was measured over the injection terminals and resulted in a sample resistance of 15 nΩ at 76 K and 0.3 nΩ at 4 K. After cutting the cable in half and terminating the two halves within a joint, a combined resistance (Terminal + Joint) of 66 nΩ

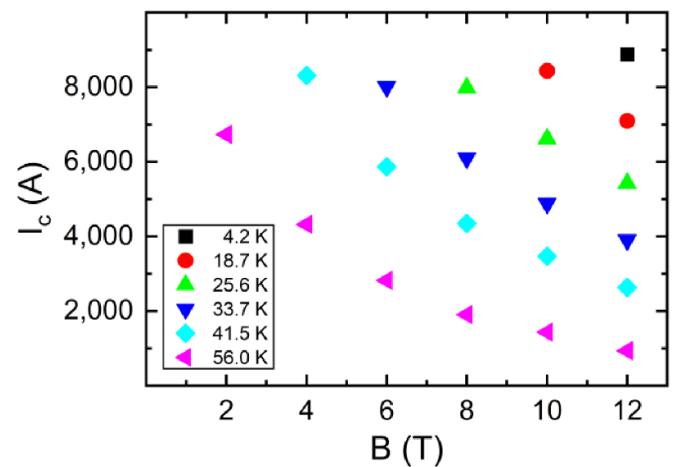


**Figure 7.** Critical current as a function of magnetic field at various temperatures of cable CORC®-30.

was measured at 76 K and of 2.2 nΩ at 4 K, as shown in figure 8.

#### 3.2. Performance of demountable joints between CORC®-CICC

Figure 9(a) shows voltage as a function of current at 76 K for the first HTS-to-HTS CICC sample pair. Figure 9(b) shows similar data for the second HTS-to-HTS sample pair with improved control of heating and copper purity. Due to

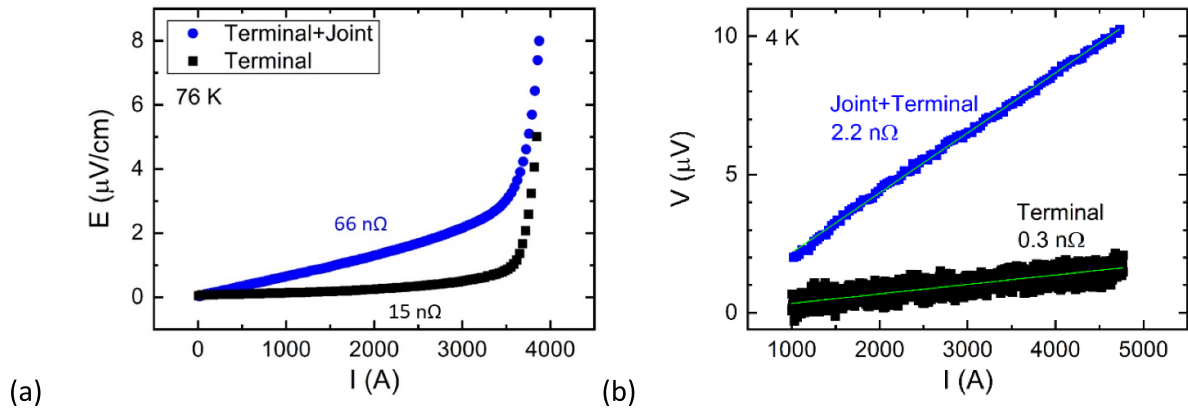


**Figure 8.** (a) Electric field as a function of current at 76 K measured across the terminations of cable CORC<sup>®</sup>-30 before and after adding the copper joint. (b) Voltage as a function of current at 4 K measured across the terminations of cable CORC<sup>®</sup>-30 before and after adding a copper joint.

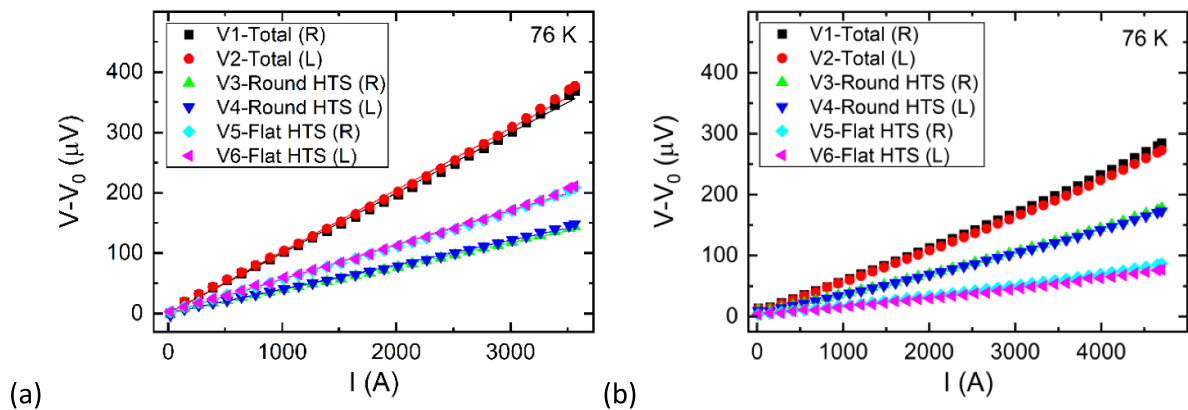


**Figure 9.** Voltage as a function of current measured at 76 K of (a) the first HTS CICC sample pair and (b) the second HTS CICC sample pair with improved control of heating and copper purity. The inductive voltage  $V_0$  caused by the current ramp rate of  $500 \text{ A s}^{-1}$  has been subtracted from the overall voltage.

**Table 2.** Average resistances of the two HTS pairs tested at 76 K.

|           |      | HTS-to-HTS pair 1 | HTS-to-HTS pair 2 |
|-----------|------|-------------------|-------------------|
| Total     | (nΩ) | 101.0             | 56.9              |
| Round HTS | (nΩ) | 39.8              | 35.8              |
| Flat HTS  | (nΩ) | 56.6              | 16.6              |
| Joint     | (nΩ) | 4.6               | 4.5               |

the improved sample preparation, the total loop resistance of the two HTS samples and the pressure joint between them decreased from 101 nΩ to 56.9 nΩ. At 76 K, most of this improvement comes from the flat HTS sample, while the joint resistance is mostly unchanged. Resistance values for both sample pairs are summarized in table 2.

The performance of the first HTS CORC<sup>®</sup>-based CICC sample pair and the pressure joint between them was measured at 4.2 K at different magnetic fields up to 8 T (figure 10). Current was increased at a rate of  $1000 \text{ A s}^{-1}$  up to 10 kA in all cases. The voltages increased linearly with current, allowing accurate determination of the resistances between the sample

terminations and the pressure contact (table 3). The terminal-to-terminal resistance of the sample decreased by a factor of 6–7 when cooled from 76 K to 4.2 K, while the contact resistance of the pressure joint decreased by a factor of more than 2 to about 2 nΩ. The decrease in resistance with temperature is caused by the drop in copper resistivity, but did not drop as much as the resistance of the joint between the single CORC<sup>®</sup> cables (figure 8) that went from 66 nΩ at 76 K to 2.2 nΩ at 4 K, which is a factor of 30. All resistances in the CICC sample increased slightly as a function of applied magnetic field, with  $R_{\text{Total}}$  increasing by 5.9 nΩ at 8 T.

The second CORC<sup>®</sup>-CICC sample pair was also tested in liquid helium at magnetic fields ranging from 0 to 8 T (figure 11), where current was increased at a rate of  $1000 \text{ A s}^{-1}$ . The contact resistance of the sample terminations was a factor of 2–8 lower (table 4) than for the first HTS-to-HTS sample pair. The results confirm that the higher quality of the copper terminations prepared with shorter heating times resulted in a drastic reduction in sample resistance. The overall resistance of the second round CORC<sup>®</sup>-CICC sample was about twice as high as that of the second flat

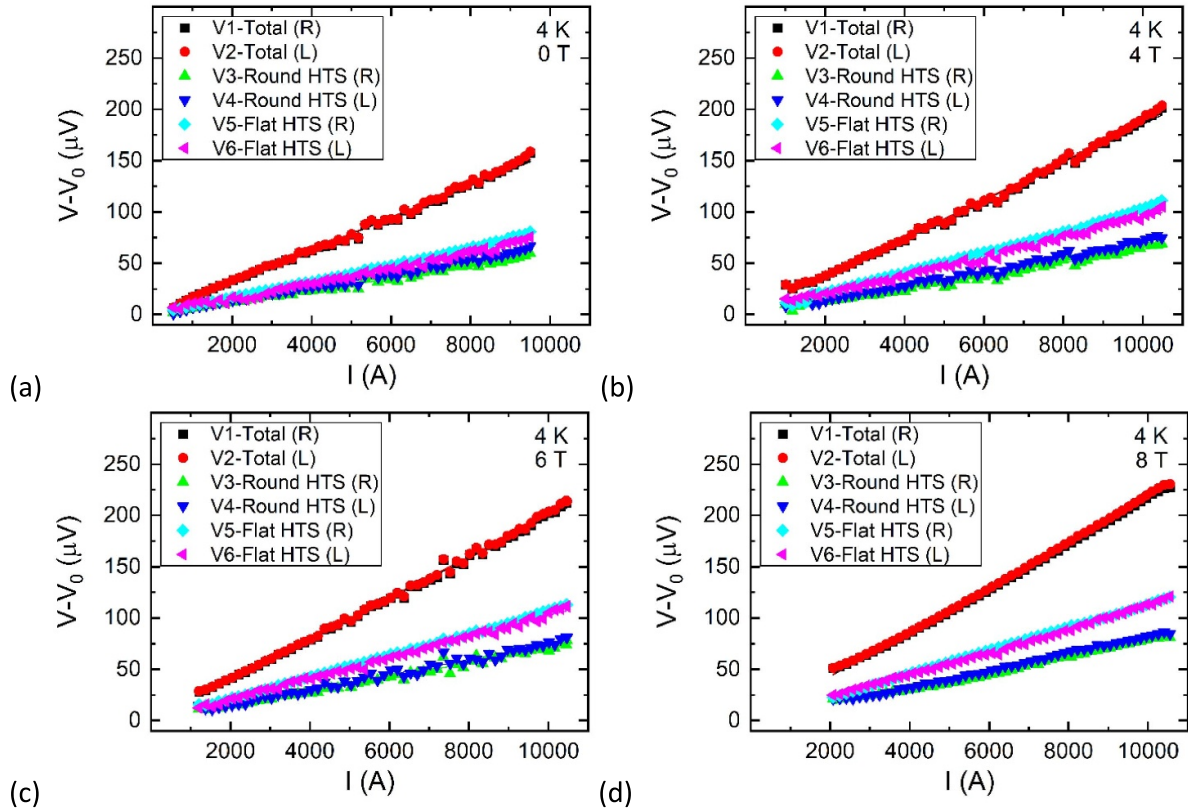


**Figure 10.** Voltage as a function of current measured at 4 K of the first HTS-to-HTS CICC sample pair. The inductive voltage  $V_0$  caused by the current ramp rate of  $1000 \text{ A s}^{-1}$  has been subtracted from the overall voltage. Measurement performed in a background magnetic field of (a) 0 T, (b) 4 T, (c) 6 T, and (d) 8 T.

**Table 3.** Resistances as a function of applied field for the first HTS-to-HTS sample pair at 4 K determined from figure 10.

| Applied field           | (T)  | 0    | 4    | 6    | 8    |
|-------------------------|------|------|------|------|------|
| $R_{\text{Total}}$      | (nΩ) | 15.8 | 18.6 | 19.9 | 21.7 |
| $R_{\text{Round HTS1}}$ | (nΩ) | 6.2  | 6.7  | 7.2  | 8.0  |
| $R_{\text{Flat HTS1}}$  | (nΩ) | 7.8  | 9.8  | 10.4 | 11.3 |
| $R_{\text{Joint}}$      | (nΩ) | 1.8  | 2.1  | 2.3  | 2.4  |

CORC<sup>®</sup>-CICC, but this is attributed to the longer current path between the terminal surface at which current is injected and the bundle of six CORC<sup>®</sup> cables. The resistance of the pressure joint was just  $0.5 \text{ n}\Omega$ , which is three times lower than that of the joint interface between the previous two CORC<sup>®</sup>-CICC samples. This is mainly attributed to the higher quality of the copper terminations that resulted in a lower resistivity at 4.2 K.

The second CORC<sup>®</sup>-CICC sample pair was also tested at 4 K at a constant current of about 4700 A for a longer time duration to determine if potential heating within the sample terminations or the joint between them would occur. The voltages did not increase within the 70 s timeframe of the measurements (figure 12). The duration of the measurements was limited due to the helium consumption of the copper bus bars at high

current. No sign of heating within the samples or the joints between them was measured. The overall sample dissipation was between 0.06 W (0 T) and 0.16 W (8 T) at a current of around 4700 A.

The final test was the joint formed by two LTS CICC samples that were identical samples, each made from three NbTi Rutherford cables. Figure 13 shows the voltage versus current measurements at 4.2 K taken at different background magnetic fields, while table 5 lists the contact resistance of the samples and that of the joint. The contact resistance of both samples is about  $1 \text{ n}\Omega$  for most fields, while that of the joint is less than  $1 \text{ n}\Omega$ . There's a relatively large uncertainty in the contact resistance of the joints, because it is calculated from the sample resistances and the overall resistance, which both are very low. Both LTS samples show a change in slope of the

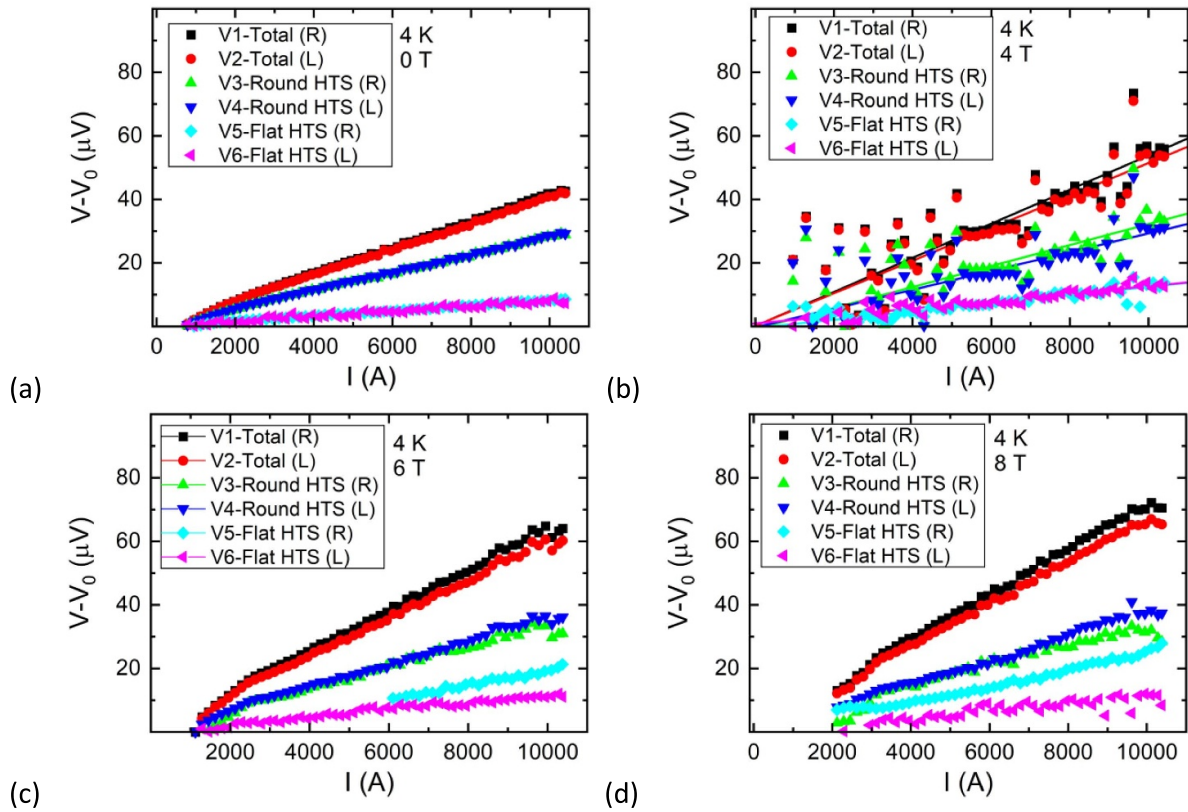


**Figure 11.** Voltage as a function of current measured at 4 K of the second HTS-to-HTS CICC sample pair. The inductive voltage  $V_0$  caused by the current ramp rate of  $1000 \text{ A s}^{-1}$  has been subtracted from the overall voltage. Measurement performed in a background magnetic field of (a) 0 T, (b) 4 T, (c) 6 T and (d) 8 T.

**Table 4.** Resistances as a function of applied field for the second HTS-to-HTS sample pair at 4 K determined from figure 11.

| Applied field           | (T)  | 0   | 4   | 6   | 8   |
|-------------------------|------|-----|-----|-----|-----|
| $R_{\text{Total}}$      | (nΩ) | 4.1 | 5.2 | 6.1 | 6.9 |
| $R_{\text{Round HTS2}}$ | (nΩ) | 2.8 | 3.0 | 3.4 | 3.6 |
| $R_{\text{Flat HTS2}}$  | (nΩ) | 0.8 | 1.3 | 1.5 | 1.9 |
| $R_{\text{Joint}}$      | (nΩ) | 0.5 | 0.9 | 1.2 | 1.4 |

$VI$ -curve at currents below 4 kA in self-field and less than 2 kA when field is applied.

## 4. Discussion

### 4.1. Importance of copper purity in CICC terminations and influence of heating time on the REBCO tape-to-tape joint resistance

The resistance of the joint between two CORC<sup>®</sup> cables presented in figure 8 was about 2 nΩ at 4 K. Connecting six cables in parallel, such as was the case in both CORC<sup>®</sup>-CICC, should reduce the overall sample resistance by as much as a factor of 6. However, the resistances measured between terminals for the HTS samples presented in table 3 of 6–8 nΩ at 4 K were

5–10 times higher than expected. These larger than expected resistances prompted evaluation of the copper used to manufacture each of the joints and evaluation of the effect of heating time on REBCO tape-to-tape contact resistance.

The resistivities of sections cut from the various copper parts of the CORC<sup>®</sup>-CICC samples were measured at room temperature, 76 K, and 4 K before and after a high temperature anneal (table 6). Surprisingly, parts used to fabricate the first round CORC<sup>®</sup>-CICC sample had a relatively high resistivity at low temperature, and an extremely low residual resistivity ratio (RRR) between room temperature and 4 K of 7–8 that did not improve on annealing. This indicates that the copper parts were not made from the specified high-purity copper, but likely an alloy of copper. Most of the other parts tested had resistivity in-line with oxygen-free copper (99.95% purity

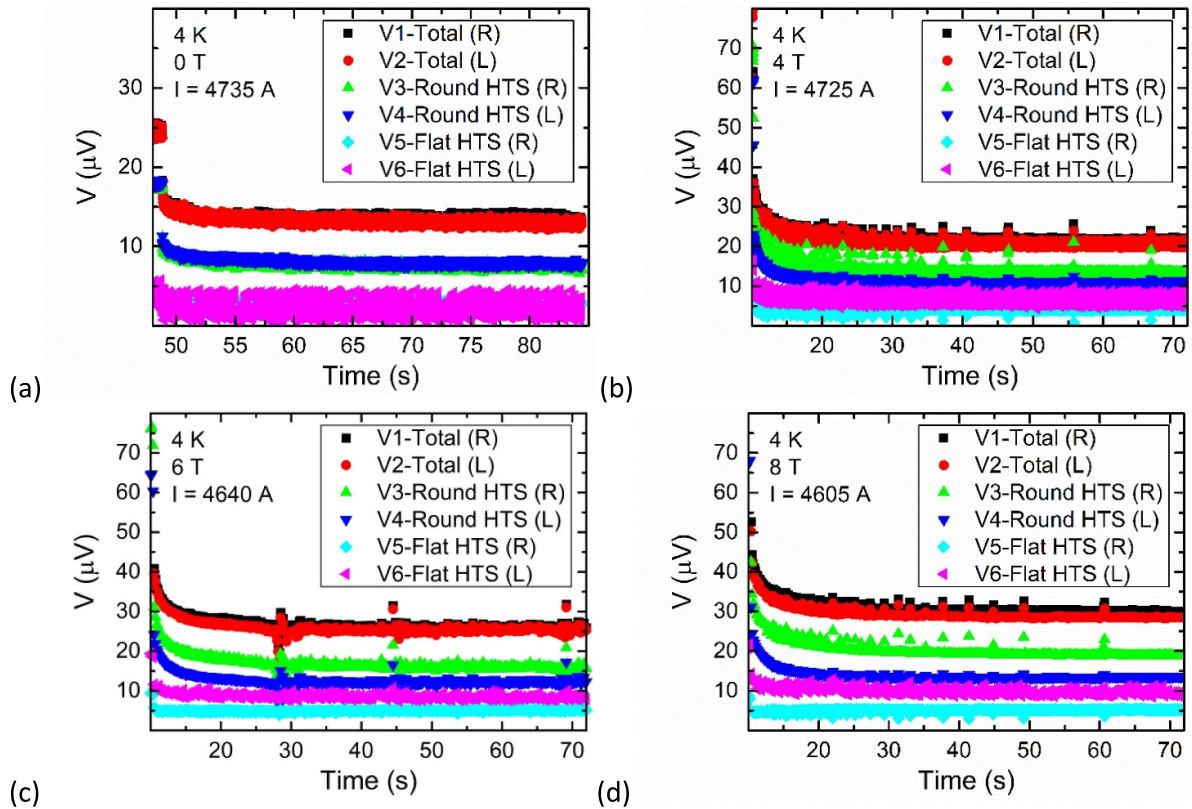


**Figure 12.** Voltage as a function of time measured at 4 K of the second HTS-to-HTS CICC sample pair when current is held constant under applied fields of (a) 0 T, (b) 4 T, (c) 6 T, and (d) 8 T. The initial voltage drop is from the decay of induced voltage due to the current ramp.

or better). The second HTS-to-HTS CICC joint pair was then manufactured using certified copper with higher purity than in the first sample pair.

Although the resistivity of the copper parts for the round CORC<sup>®</sup>-CICC sample was relatively high, the resistance of the joint between the two CORC<sup>®</sup>-CICC samples was only 2–4 times higher than that of the joint between the two LTS CICC samples. Also, the resistance of the termination of the flat CORC<sup>®</sup>-CICC was much higher than expected, while the copper components used in that sample had a very low resistivity and high RRR. This indicates that the high resistance of the CORC<sup>®</sup>-CICC terminations had another origin.

The potential cause of high contact resistance between soldered REBCO tapes due to heating was outlined in a recent talk presented by Iole Faloria at CERN [17], where she discussed the increase in contact resistivity ( $R_c$ ) between the REBCO layer and the copper plating of typical REBCO coated conductors with heating temperature and time. This study showed an increase in resistance by a factor of 1.5–2 of lap joints between REBCO tapes prepared with SnPb and SnIn solder in as little as 20 min at 170 °C–200 °C. The mechanism has been identified as oxygen-out diffusion from the REBCO to silver interface that has minimal effect on  $I_c$  for moderate heating temperatures and times, but much more substantial effect on  $R_c$  [18].

Typical CORC<sup>®</sup> terminals are heated for durations of 5–10 min using pure indium solder. However, due to their large

mass, the first HTS CICC samples were heated significantly longer (20–40 min). To determine the increase in joint resistivity with heating temperature and time, lap joints between two REBCO tapes were prepared by soldering two tapes together at either 175 °C, or 200 °C for 1.5, 5 and 15 min (see figure 1). The performance of the lap joints was measured at 76 K, (figure 14), where a large increase in contact resistance was measured once the heating time exceeded 5 min. An increase in joint resistivity of a factor of 2–4 was measured (table 7) after just 15 min of heating, while the critical current and  $n$ -value of the tapes remained unchanged.

The results outlined in this section have a major impact on the quality and performance of CORC<sup>®</sup> cable, wire, and CICC terminations. The increase in  $R_c$  with heating time likely originates from one of the internal interfaces within the REBCO tape such as the REBCO-to-silver interface, where oxygen diffuses out from the REBCO film, through the silver cap layer, and into the copper that acts as a sink for oxygen [17, 18]. This results in an increase in resistance when HTS terminations are heated to make their soldered connections. The increase in resistivity with soldering time can also cause  $R_c$  between individual CORC<sup>®</sup> cables and the termination of a CORC<sup>®</sup>-CICC to vary in larger joint structures because the local temperature and time experienced at high temperature may vary across the structure. This could potentially cause an inhomogeneous current distribution between CORC<sup>®</sup> cables within the CORC<sup>®</sup>-CICC. It is therefore vital for the successful operation of

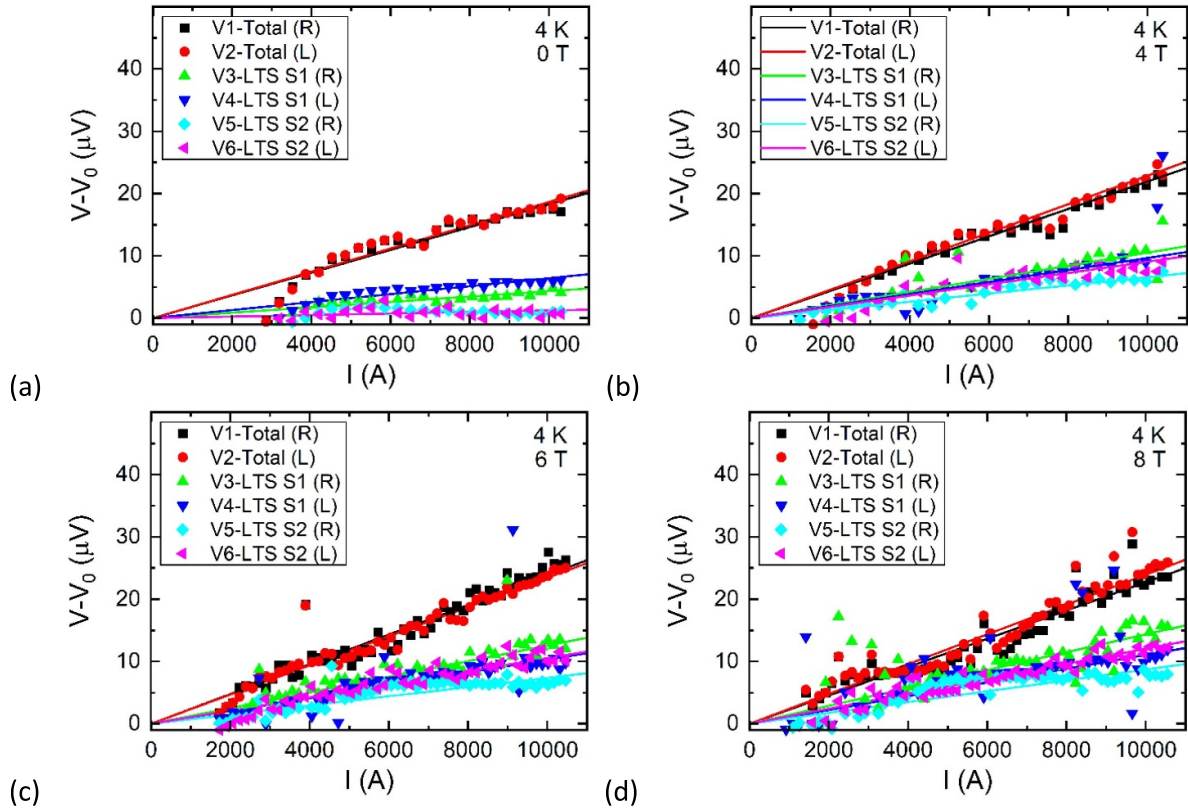


**Figure 13.** Voltage as a function of current measured at 4 K of the LTS-to-LTS CICC sample pair. The inductive voltage  $V_0$  caused by the current ramp rate of  $1000 \text{ A s}^{-1}$  has been subtracted from the overall voltage. Measurement performed in a background magnetic field of (a) 0 T, (b) 4 T, (c) 6 T, and (d) 8 T.

**Table 5.** Resistances as a function of applied field for the LTS-to-LTS CICC sample pair at 4 K determined from figure 13.

| Applied field       | (T)  | 0   | 4   | 6   | 8   |
|---------------------|------|-----|-----|-----|-----|
| $R_{\text{Total}}$  | (nΩ) | 1.8 | 2.2 | 2.4 | 2.3 |
| $R_{\text{LTS S1}}$ | (nΩ) | 0.5 | 1.0 | 1.1 | 1.3 |
| $R_{\text{LTS S2}}$ | (nΩ) | 0.1 | 0.8 | 0.9 | 1.0 |
| $R_{\text{Joint}}$  | (nΩ) | 1.2 | 0.4 | 0.4 | 0.0 |

CORC<sup>®</sup>-CICC that the heating time during soldering is minimized to less than 10 min.

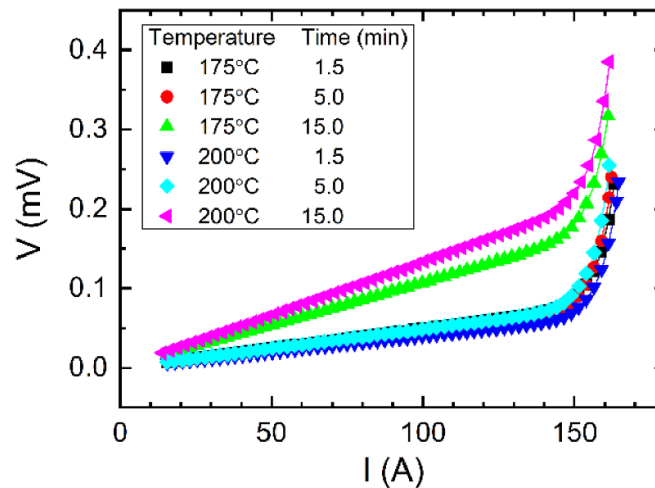
#### 4.2. Influence of magnetic field on the resistance of CICC joints

While demountable joints in fusion reactors will need to be operated in high magnetic fields, little data has been published on the magnetoresistance of demountable HTS CICC joints. Magnetoresistance in copper depends largely on material purity [22], while soldered REBCO tapes have only slight (2%–15%) change of joint resistivity with applied fields up to 8 T [23, 24]. Contact resistance between HTS CICC sample pairs joined together using indium tested in the Sultan test facility in a stray field of 1–4 T at 5 K have been reported for 300 mm long CORC<sup>®</sup> CICC joints (3.3 nΩ) [11, 25] and 400 mm long VIPER CICC joints (1.3–5.5 nΩ) [26].

For pressed Cu-to-Cu contacts, resistivities at 4.2 K have been reported on the order of 5–1000 nΩcm<sup>2</sup> [27–30] depending on surface quality and applied pressure. The joints between CICC's studied here had a contact area of  $61 \times 150 \text{ mm}$  and a contact pressure of 10–100 MPa. Therefore, a contact resistivity of about 100 nΩcm<sup>2</sup> would be expected between our CICC sample pairs, resulting in a resistance around 1.1 nΩ. This is close to the values measured in the three tests where  $R_{\text{Joint}}$  ranged between 0.5 and 1.8 nΩ. For the HTS-to-HTS sample pairs, there was a magnetoresistance effect where  $R_{\text{Joint}}$  increased as a function of applied field by 0.6–0.9 nΩ at 8 T. Such an effect was not observed in the LTS-to-LTS sample pair. The higher magnetoresistance observed is likely because of the additional copper between the superconducting part of the HTS sample pairs. The HTS-to-HTS sample pair had a center-to-center distance between the two CICC legs of 21 mm while separation between Rutherford cables in the two legs of

**Table 6.** Resistivity and residual resistivity ratio (RRR) of the various copper components of the CORC® samples. Copper sections were cut from the joint sections for the indicated CICC samples.

| Part                       | Temper       | Resistivity  |             |            | RRR (293 K/4 K) |
|----------------------------|--------------|--------------|-------------|------------|-----------------|
|                            |              | 293 K (nΩ m) | 76 K (nΩ m) | 4 K (nΩ m) |                 |
| 1/8 hard C101 copper wire  | H00 (1/8 CW) | 17.08        | 1.93        | 0.08       | 225             |
| Half-hard C101 copper wire | H02 (1/2 CW) | 16.73        | 2.15        | 0.20       | 85              |
| 20 cm single CORC® joint   | Annealed     | 18.73        | 2.19        | 0.13       | 148             |
| First round CORC® CICC     | As-received  | 19.36        | 4.55        | 2.61       | 7               |
| First round CORC® CICC     | Annealed     | 18.14        | 4.30        | 2.38       | 8               |
| Second round CORC® CICC    | As-received  | 18.68        | 2.50        | 0.40       | 47              |
| Second round CORC® CICC    | Annealed     | 17.36        | 1.94        | 0.05       | 356             |
| First flat CORC® CICC      | As-received  | 18.20        | 2.19        | 0.20       | 90              |
| First flat CORC® CICC      | Annealed     | 17.90        | 2.02        | 0.06       | 305             |
| Second flat CORC® CICC     | As-received  | 17.96        | 2.47        | 0.48       | 37              |
| Second flat CORC® CICC     | Annealed     | 17.64        | 2.16        | 0.25       | 70              |
| LTS CICC -S1               | As-received  | 17.83        | 2.25        | 0.22       | 83              |
| LTS CICC -S1               | Annealed     | 17.52        | 1.96        | 0.07       | 257             |
| LTS CICC-S2                | As-received  | 18.19        | 2.28        | 0.23       | 79              |
| LTS CICC-S2                | Annealed     | 16.82        | 1.93        | 0.06       | 269             |

**Figure 14.** Voltage as a function of current for REBCO-to-REBCO lap-joints soldered at different temperatures for various durations.**Table 7.** Performance of lap joints between two REBCO tapes at 76 K.

| Sample # | Heating temp (°C) | Time (min) | $R$ (nΩ) | $R_c$ (nΩ cm <sup>2</sup> ) | $I_c$ (A) | $n$ -value |
|----------|-------------------|------------|----------|-----------------------------|-----------|------------|
| 1        | 175               | 1.5        | 501      | 401                         | 146       | 29.5       |
| 2        | 175               | 5.0        | 445      | 356                         | 145       | 29.4       |
| 3        | 175               | 15.0       | 1074     | 859                         | 144       | 28.0       |
| 4        | 200               | 1.5        | 398      | 318                         | 147       | 28.5       |
| 5        | 200               | 5.0        | 492      | 394                         | 144       | 29.4       |
| 6        | 200               | 15.0       | 1337     | 1069                        | 144       | 29.6       |

the LTS-to-LTS sample pair was only 9 mm. For the LTS pairs,  $R_{\text{Joint}}$  decreases with applied field. This anomaly may be a consequence of where voltage is being measured, on either side of the sample, that could be at a slightly different voltage potential than close to the Rutherford cables where more current is flowing. Future work should include modeling of current distribution across the pressed interface of the different CICC configurations.

## 5. Conclusion

The development of compact fusion machines relies on the development of low resistance joints between high-current HTS cables and CICC. Resistances as low as 51 nΩ at 76 K and 1.9 nΩ at 4.2 K were measured between two 6.8 mm thick CORC® cables containing 30 REBCO tapes in a compact joint measuring just 16 × 38 × 200 mm. To study the feasibility

of demountable Cu-to-Cu dry contact joints made between CICC samples, two CORC<sup>®</sup>-based layouts, one round six-cable CICC and one flat six-cable CICC, were designed using 12-tape CORC<sup>®</sup> cables. A clamping structure was developed and tested to ensure at least 10 MPa clamping pressure over the entire joint area measuring just 61 × 150 mm. Initial testing revealed higher resistances than expected that were attributed to heating times exceeding 20 min to solder the CORC<sup>®</sup> cables into their terminations. More detailed experiments showed that the internal contact resistance within the REBCO tapes increases by a factor of 2–4 when heated for 15 min, likely because of oxygen diffusion out of the REBCO layer.

A second sample pair manufactured with faster soldering times achieved significantly lower resistance, with a total loop resistance (including both HTS samples' injection and joint terminations and the Cu-to-Cu interface between them) of 56.9 nΩ at 76 K and 4.1 nΩ at 4 K. The joint resistance was found to contribute only 4.6 nΩ at 76 K and 0.5 nΩ at 4 K. Both the total loop resistance and joint resistance at 4 K increased to 6.9 and 1.4 nΩ, respectively, when a magnetic field of 8 T was applied. Most of the resistance came from the round CICC configuration that contained more copper between the superconducting CORC<sup>®</sup> cables and the joint interface, while the flat CICC configuration contributed 0.8 and 1.9 nΩ at 0 and 8 T respectively. This is comparable to an LTS-to-LTS CICC consisting of three NbTi Rutherford cables that was tested with a resistance of 0.5 and 1.3 nΩ at 0 T and 8 T respectively. The results demonstrate the feasibility of developing CORC<sup>®</sup>-CICC joints based on dry copper-to-copper contacts with sufficiently low resistance needed for demountable fusion coils. The overall joint resistance of 4.1 nΩ at 4 K resulted in a dissipation of only 0.4 W at 10 kA but would increase to about 10 W per joint at an operating current of 50 kA. The joint resistance could easily be reduced further by increasing the joint length, and by terminating the CORC<sup>®</sup>-CICC in a flat, instead of a round configuration.

### Data availability statement

All data that support the findings of this study are included within the article (and any supplementary files).

### Acknowledgments

This work was in part supported by the US Department of Energy under Agreement Nos. DE-SC0013723, DE-SC0014009, DE-SC0018125 and DE-SC0019934. Part of this work has been funded by STEP, a UKAEA program to design and build a prototype fusion energy plant and a path to commercial fusion.

### ORCID iDs

Jeremy D Weiss  <https://orcid.org/0000-0003-0026-3049>  
 Danko C van der Laan  <https://orcid.org/0000-0001-5889-3751>  
 Nadezda Bagrets  <https://orcid.org/0000-0003-0323-4972>

### References

- [1] Mitchell N *et al* 2021 Superconductors for fusion: a roadmap *Supercond. Sci. Technol.* **34** 103001
- [2] Sorbom B N *et al* 2015 ARC: a compact, high-field, fusion nuclear science facility and demonstration power plant with demountable magnets *Fusion Eng. Des.* **100** 378–405
- [3] Commonwealth Fusion Systems (available at: <https://cfs.energy/>) (Accessed 29 June 2022)
- [4] Tokamak Energy Tokamak Energy (available at: [www.tokamakenergy.co.uk/](http://www.tokamakenergy.co.uk/)) (Accessed 29 June 2022)
- [5] Tri Alpha Energy Technologies (available at: <https://tae.com/>) (Accessed 29 June 2022)
- [6] Buckingham R and Loving A 2016 Remote-handling challenges in fusion research and beyond *Nat. Phys.* **12** 5
- [7] VLT 2020 VLT 21 January (available at: <https://vlt.ornl.gov/research/082714VLTkessel.pdf>) (Accessed 29 June 2022)
- [8] UKAEA GOV.UK (available at: [www.gov.uk/government/speeches/making-science-work-together-how-can-we-build-the-best-possible-future-for-science-research-and-innovation-in-the-uk](http://www.gov.uk/government/speeches/making-science-work-together-how-can-we-build-the-best-possible-future-for-science-research-and-innovation-in-the-uk)) (Accessed 29 June 2022)
- [9] Bajko M *et al* 2009 Report of the task force on the incident of 19th September 2008 at the LHC CERN-LHC-PROJECT-REPORT-1168
- [10] van der Laan D C, Weiss J D and McRae D M 2019 Status of CORC<sup>®</sup> cables and wires for use in high-field magnets and power systems a decade after their introduction *Supercond. Sci. Technol.* **32** 033001
- [11] Mulder T, Weiss J, Van Der Laan D, Dudarev A and Ten Kate H 2020 Recent progress in the development of CORC<sup>®</sup> cable-in-conduit conductors *IEEE Trans. Appl. Supercond.* **30** 4800605
- [12] Mulder T, Dudarev A, van der Laan D C, Mentink M G T, Dhallé M and ten Kate H H J 2015 Optimized and practical electrical joints for CORC type HTS cables *IOP Conf. Ser.: Mater. Sci. Eng.* **102** 012026
- [13] Mulder T, van der Laan D, Weiss J D, Dudarev A, Dhallé M and ten Kate H H J 2017 Design and preparation of two REBCO-CORC<sup>®</sup> cable-in-conduit conductors for fusion and detector magnets *IOP Conf. Ser.: Mater. Sci. Eng.* **279** 012033
- [14] van der Laan D C Superconducting cable connections and methods US20160352027A1 01 December 2016 (available at: <https://patents.google.com/patent/US20160352027/en>) (Accessed 8 July 2019)
- [15] Mulder T, Fleiter J, Willering G, Dudarev A, Mentink M, Dhalle M and Kate H T 2017 Demonstration of the REBCO CORC<sup>®</sup> 47kA@10T/4.2K cable-in-conduit-conductor and its joint terminals at 4.5 and 77 K *IEEE Trans. Appl. Supercond.* **27** 4801004
- [16] Willering G P, van der Laan D C, Weijers H W, Noyes P D, Miller G E and Viouchkov Y 2015 Effect of variations in terminal contact resistances on the current distribution in high-temperature superconducting cables *Supercond. Sci. Technol.* **28** 3

- [17] Falorio I Effect of heating time and temperature on joint resistance of REBCO tapes TE-MSC-SCD (14 June 2020)
- [18] Lu J, Xin Y, Jarvis B and Bai H 2021 Oxygen out-diffusion in REBCO coated conductor due to heating *Supercond. Sci. Technol.* **34** 075004
- [19] Weiss J D, van der Laan D C, Hazelton D, Knoll A, Carota G, Abrahimov D, Francis A, Small M A, Bradford G and Jaroszynski J 2020 Introduction of the next generation of CORC<sup>®</sup> wires with engineering current density exceeding  $650 \text{ A mm}^{-2}$  at 12 T based on SuperPower's REBCO tapes containing substrates of  $25 \mu\text{m}$  thickness *Supercond. Sci. Technol.* **33** 044001
- [20] Barth C, van der Laan D C, Bagrets N, Bayer C M, Weiss K-P and Lange C 2015 Temperature- and field-dependent characterization of a conductor on round core cable *Supercond. Sci. Technol.* **28** 065007
- [21] SuperPower 2G HTS wire specification (available at: [www.superpower-inc.com/specification.aspx](http://www.superpower-inc.com/specification.aspx)) (Accessed 28 September 2022)
- [22] Fickett F R Magnetoresistivity of copper and aluminum at cryogenic temperatures (available at: <https://lss.fnal.gov/conf/C720919/p539.pdf>)
- [23] Fleiter J and Ballarino A 2017 In-field electrical resistance at 4.2 K of REBCO splices *IEEE Trans. Appl. Supercond.* **27** 4
- [24] Tsui Y, Surrey E and Hampshire D 2016 Soldered joints—an essential component of demountable high temperature superconducting fusion magnets *Supercond. Sci. Technol.* **29** 7
- [25] Mulder T 2018 Advancing REBCO-CORC wire and cable-in-available at: conduit conductor technology for superconducting magnets (<https://doi.org/10.3990/1.9789036546164>)
- [26] Hartwig Z S *et al* 2020 VIPER: an industrially scalable high-current high-temperature superconductor cable *Supercond. Sci. Technol.* **33** 11LT01
- [27] Noterdaeme J-M 1977 Demountable resistive joint design for high current superconductors. *Master's Thesis* MIT
- [28] Nilles M J Thermal and electrical contact resistance of OFHC copper from 4k to 290k (low temperature, cryogenics, pressed contacts, contact conductance) *PhD thesis* The University of Wisconsin—Madison, Wisconsin (available at: [www.proquest.com/docview/303433259/abstract/9C1B39C4D2124B22PQ/1](http://www.proquest.com/docview/303433259/abstract/9C1B39C4D2124B22PQ/1)) (Accessed 15 February 2022)
- [29] Vansciver S W N 1985 Thermal and electrical contact conductance studies (available at: <https://ntrs.nasa.gov/search.jsp?R=19860021906>) (Accessed 26 June 2020)
- [30] Zar J L 1995 Electrical switch contact resistance at 4.2°K *Advances in Cryogenic Engineering* (Boston, MA: Springer) pp 95–101